ORIGINAL ARTICLE

Synaptotagmin-11 inhibits spontaneous neurotransmission through vti1a

Wan-Ru Li[1] | Ya-Long Wang[1] | Chao Li[2,3] | Pei Gao[1] | Fei-Fan Zhang[1] | Meiqin Hu[4] | Jing-Chen Li[1] | Shuli Zhang[2,3] | Rena Li[5] | Claire Xi Zhang[1,6] [ID]

[1]Beijing Institute of Brain Disorders, Laboratory of Brain Disorders, Ministry of Science and Technology, Collaborative Innovation Center for Brain Disorders, Capital Medical University, Beijing, China

[2]State Key Laboratory of Brain and Cognitive Sciences, Institute of Biophysics, Chinese Academy of Sciences, Beijing, China

[3]University of Chinese Academy of Sciences, Beijing, China

[4]Department of Molecular, Cellular, and Developmental Biology, University of Michigan, Ann Arbor, Michigan, USA

[5]Beijing Key Laboratory of Mental Disorders, Beijing Anding Hospital and Beijing Institute of Brain Disorders, Capital Medical University, Beijing, China

[6]Academy of Pharmacy, Xi'an Jiaotong-Liverpool University, Suzhou, China

Correspondence
Rena Li, Beijing Key Laboratory of Mental Disorders, Beijing Anding Hospital and Beijing Institute of Brain Disorders, Capital Medical University, Beijing, China.
Email: renali@ccmu.edu.cn

Claire Xi Zhang, Beijing Institute of Brain Disorders, Laboratory of Brain Disorders, Ministry of Science and Technology, Collaborative Innovation Center for Brain Disorders, Capital Medical University, Beijing, China.
Email: clairexizhang@ccmu.edu.cn

Funding information
National Natural Science Foundation of China, Grant/Award Number: 31471085, 91849103 and 81671248; Beijing Natural Science Foundation Program and Scientific Research Key Program of Beijing Municipal Commission of Education, Grant/Award Number: KZ201510025023

Abstract

Recent work has revealed that spontaneous release plays critical roles in the central nervous system, but how it is regulated remains elusive. Here, we report that synaptotagmin-11 (Syt11), a Ca^{2+}-independent Syt isoform associated with schizophrenia and Parkinson's disease, suppressed spontaneous release. Syt11-knockout hippocampal neurons showed an increased frequency of miniature excitatory post-synaptic currents while over-expression of Syt11 inversely decreased the frequency. Neither knockout nor over-expression of Syt11 affected the average amplitude, suggesting the pre-synaptic regulation of spontaneous neurotransmission by Syt11. Glutathione S-transferase pull-down, co-immunoprecipitation, and affinity-purification experiments demonstrated a direct interaction of Syt11 with vps10p-tail-interactor-1a (vti1a), a non-canonical SNARE protein that maintains spontaneous release. Importantly, knockdown of vti1a reversed the phenotype of Syt11 knockout, identifying vti1a as the main target of Syt11 inhibition. Domain analysis revealed that the C2A domain of Syt11 bound vti1a with high affinity. Consistently, expression of the C2A domain alone rescued the phenotype of elevated spontaneous release in Syt11-knockout neurons similar to the full-length protein. Altogether, our results suggest that Syt11 inhibits vti1a-containing vesicles during spontaneous release.

KEYWORDS
SNARE, spontaneous release, synaptotagmin, vti1a

1 | INTRODUCTION

Spontaneous neurotransmission at the frog neuromuscular junction was initially discovered by Fatt and Katz about 70 years ago (Fatt & Katz, 1950, 1952). Since then, it has been found in every type of synapse under physiological conditions in which neurotransmitter is released at a low frequency. Accumulating evidence points to important functions of spontaneous release, including post-synaptic signal transduction, guiding the maturation of primeval synapses, and mediating synaptic plasticity (Kavalali, 2015).

The molecular mechanisms underlying spontaneous release are less well understood than action potential-evoked release and it has been a long-standing question as to whether and how they are related (Kaeser & Regehr, 2014; Truckenbrodt & Rizzoli, 2014). Considerable evidence supports the idea that they are driven by either the same vesicle pool or separate pools (Cornelisse et al., 2012; Fredj & Burrone, 2009; Groemer & Klingauf, 2007; Hua et al., 2011; Ikeda & Bekkers, 2009; Mathew et al., 2008; Sara et al., 2005). Recent studies have revealed some molecular distinctions between these two types of neurotransmission (Andreae & Burrone, 2018; Gonzalez-Islas et al., 2018; Kavalali, 2018; Williams & Smith, 2018). While evoked and spontaneous neurotransmission are predominantly mediated by the canonical SNARE complex comprising synaptobrevin2 (syb2, also named VAMP2), syntaxin1, and SNAP-25 (Sudhof & Rothman, 2009), some of the spontaneous neurotransmitter release is mediated by alternative vesicular SNARE proteins, such as VAMP7, vps10p-tail-interactor-1a (vti1a), and to some degree VAMP4 (Bal et al., 2013; Crawford et al., 2017; Hua et al., 2011; Kononenko & Haucke, 2012; Raingo et al., 2012; Ramirez et al., 2012). Among them, vti1a is trafficked most robustly at rest and promotes high-frequency spontaneous release (Ramirez et al., 2012). Loss of both syb2 and vti1a markedly diminishes high-frequency spontaneous neurotransmission, suggesting that syb2- and vti1a-containing vesicles are mainly responsible for spontaneous release. Vti1a belongs to a family of SNARE proteins that regulate endolysosomal trafficking and are conserved from yeast to human (Emperador-Melero et al., 2019). Vti1a and vti1b, mammalian genes universally expressed in all tissues (Advani et al., 1998), play largely redundant roles in regulating protein sorting at the Golgi, and they are also required for synaptic transmission and dense-core vesicle secretion (Emperador-Melero et al., 2018, 2019; Walter et al., 2014). Vti1a, but not vti1b, is localized at synapses and in synaptic vesicle fractions (Antonin et al., 2002; Takamori et al., 2006), supporting its unique role in spontaneous neurotransmission (Crawford et al., 2017; Kononenko & Haucke, 2012; Ramirez et al., 2012).

Besides the molecular distinction in the SNARE complex, spontaneous neurotransmission is also differentially regulated by SNARE-binding proteins (such as synaptotagmins, complexin, double C2-domain containing protein, and copine6), neuromodulators, and other signaling pathways compared to evoked neurotransmitter release (Fawley et al., 2014; Glitsch, 2006; Groffen et al., 2010; Huntwork & Littleton, 2007; Maximov & Sudhof, 2005; Pang et al., 2011; Pratt et al., 2011; Schupp et al., 2016; Xu et al., 2009; Yang et al., 2013).

In this study, we investigated the function of synaptotagmin-11 (Syt11), a Ca^{2+}-independent syt isoform essential for mouse development (von Poser et al., 1997; Shimojo et al., 2019), in spontaneous neurotransmission. Syt11 is a risk locus for Parkinson's disease and a candidate gene for susceptibility to schizophrenia (Huynh et al., 2003; Inoue et al., 2007; International Parkinson Disease Genomics Consortium et al., 2011; Pihlstrom et al., 2013; Sesar et al., 2016). It belongs to the syt family, which is known for its roles in evoked and/or spontaneous neurotransmission (Pang & Sudhof, 2010). Syt1, Syt2, and Syt9 all act as Ca^{2+} sensors to promote evoked neurotransmission but clamp spontaneous release (Bacaj et al., 2013; Geppert et al., 1994; Liu et al., 2009; Maximov & Sudhof, 2005; Nishiki & Augustine, 2004; Pang et al., 2006; Sun et al., 2007; Wierda & Sorensen, 2014; Xu et al., 2007, 2009). Syt4, which is most homologous with Syt11 and does not bind Ca^{2+} biochemically either, suppresses spontaneous release without affecting evoked exocytosis (Dean et al., 2009). In contrast, Syt12, also a non-Ca^{2+} binding Syt, selectively promotes spontaneous release, leaving evoked neurotransmission unaltered (Maximov et al., 2007). Therefore, different Syt family members play distinct roles in spontaneous release, most likely because of unique protein–protein and/or protein–lipid interactions. Syt11 plays multiple roles in membrane trafficking in neurons and glia (Bento et al., 2016; Du et al., 2017; Shimojo et al., 2019; Sreetama et al., 2016; Wang et al., 2016, 2018; Yan et al., 2020). It regulates neuronal endocytosis, the autophagy–lysosome pathway, and synaptic plasticity; functions in lysosome exocytosis for membrane repair, caveolae-mediated endocytosis, and mechanoprotection in astrocytes; and inhibits phagocytosis and cytokine release in microglia. We previously reported that Syt11 inhibits clathrin-mediated and bulk endocytosis without affecting evoked exocytosis (Wang et al., 2016). Recently, Shimojo et al. reported that Syt11 does not regulate evoked neurotransmission, and does not bind the canonical SNARE complex (Shimojo et al., 2019). Interestingly, a study of Syt11-interacting partners in β cells showed that vti1a can be pulled down by glutathione S-transferase (GST)-Syt11 (Milochau et al., 2014). Therefore, we hypothesized that Syt11 may regulate spontaneous release *via* vti1a-containing vesicles.

2 | MATERIALS AND METHODS

2.1 | Reagents

The primary antibodies for western blots, immunofluorescence, and co-immunoprecipitation assays were anti-Syt11 (Synaptic Systems, Cat# 270003, RRID:AB_2619994, working dilution: 1:500–1000), anti-Syb2 (Synaptic Systems, Cat# 104211, RRID:AB_887811, 1:1000), anti-Vti1a (BD Biosciences, Cat# 611220, RRID:AB_398752, 1:1000), anti-c-Myc (Santa Cruz Biotechnology, Cat# sc-42, RRID:AB_2282408, 1:5000), mouse normal IgG (Millipore, Cat# 12–371, RRID:AB_145840, 1:250), rabbit normal IgG (Millipore, Cat# 12–370, RRID:B_145841, 1:250), anti-GAPDH (Sigma-Aldrich, Cat# G8795, RRID:AB_1078991, 1:10000), and anti-His (Absin Bioscience Inc., Cat# 830002 (2019),

1:1000). All cell culture media were from Hyclone. Chemicals were from Sigma unless stated otherwise.

2.2 | Animals

The floxed Syt11 knock-in mice were from The Jackson Laboratory (stock number 008294, strain B6.129-Syt11$^{tm1Sud/J}$, purchased in 2011). This strain was genotyped using the specific forward primer 5'-AATCTCAGCACTCAGGAGTCAG-3' and reverse primer 5'-CTCTTGCTTACTGATTGGCAGC-3'. PCR was performed at an annealing temperature of 57°C (1 min) and extension at 72°C (1 min) for 35 cycles. The Syt11 knock-in homozygote showed a 500-bp band and wild-type mice and a 361-bp band. The Syt11 gene was silenced using cre recombinase. The animals were housed with free access to food and water *ad libitum*. The care and use of animals were approved and directed by the Animal Care and Use Committee of Capital Medical University (protocol# AEEI-2015–124). The study was not pre-registered. Neither randomization nor blinding was performed in this study.

2.3 | Cell culture

Hippocampi were dissected from 1- to 2-day-old floxed Syt11 knock-in mice or C57BL/6 mice under hypothermia. Neurons were dissociated with trypsin (0.25 mg/ml for 15 min at 37°C), then triturated with a 2-ml Pasteur pipette, and plated on 2.5-cm coverslips coated with poly-D-lysine (Sigma-Aldrich, Cat# 0899 (2017)). One mouse was used for every three coverslips. The culture medium consisted of 96% Neurobasal-a, 2% B-27 supplement, and 2% Glutamax. Cultures were maintained at 37°C in a humidified incubator gassed with 95% air and 5% CO_2. All cultured neuron experiments were performed at 14–16 days *in vitro* (DIV).

2.4 | Lentiviral preparation

Lentivirus was prepared by transfecting the pFUGW plasmid with genes of interest and three helper plasmids pRev, pRRE, and pVSVG (expressing viral packaging and coating proteins) into human embryonic kidney (HEK) 293-T cells (ATCC®, Cat# CRL-3216™, RRID:CVCL_0063) (this cell line is not listed as a commonly misidentified cell line by the International Cell Line Authentication Committee). No further authentication was performed in the laboratory. A maximum of five cell passages was used. The virus was harvested from the culture medium 48 h after transfection. Primary cultured hippocampal neurons were infected with lentivirus at DIV4 or twice at DIV4 and DIV5. The infection efficiency was ~90%.

The cre- and Δcre-expressing lentivirus plasmids were a kind gift from Dr. Chen Zhang (Capital Medical University). They contained enhanced green fluorescent protein (EGFP) followed by a nuclear localization signal (NLS) and the cre or Δcre recombinase sequence (EGFP-NLS-CRE/ΔCRE).

The hairpin shRNA sequences used to knock down vti1a in primary cultured hippocampal neurons were as follows: sense 5'-GGGCACATCTGCTGGATAA-3' (vti1a KD-1) and sense 5'-GCAGTGGAGACTGAGCAAA-3' (vti1a KD-2). A random sequence (sense 5'-TTCTCCGAACGTGTCACGT-3') that was predicted not to target any genes in mouse cells served as a negative control (Shanghai Obio Technology Corp., Ltd.).

For over-expression and rescue experiments, lentivirus expressing myc-Syt11-IRES2-BFP or myc-C2A-IRES2-BFP was used. Three copies of c-myc tag (GAGCAGAAGCTGATCAGTGAAGAGGACTTG in the DNA sequence) and a linker region (GGCAGCGGTAGT) were tagged to the N-terminal of the mouse Syt11 gene.

2.5 | Electrophysiology

All data were acquired by a HEKA USB10 amplifier and PatchMaster software (Lambrecht/Pfalz, HEKA USB10, RRID:SCR_000034). For mEPSC recording, the external bath solution contained (in mM) 150 NaCl, 4 KCl, 2 $MgCl_2$, 2 $CaCl_2$, 10 glucose, and 10 HEPES (pH 7.4, adjusted with NaOH). For isolation of miniature EPSCs (mEPSCs), tetrodotoxin (TTX, 1 μM) (Apexbio, Cat# N1671 (2017)) and the $GABA_A$ receptor blocker bicuculline (20 μM) (Selleck, Cat# s7071 (2017)) were added. The pipette solution contained (in mM) 135 CsCl, 10 HEPES, 1 EGTA, 1 Na-GTP, 4 Mg-ATP, and 10 QX-314 (Alomone Labs, Cat# Q100Q16500 (2017)) (pH 7.4, adjusted with CsOH). All the mEPSC events were recorded at a holding potential of −70 mV. Pipettes (Sutter Instrument, Cat# BF-150–110-10HP (2017)) used in recording had a resistance of 3–5 MΩ. Neurons with a leak current >200 pA were discarded. mEPSC frequencies were analyzed by Mini Analysis Software (RRID:SCR_002184) (search parameters: gain: 20; blocks: 3940; threshold (pA): 20; period to search for a local maximum (μs): 20000; time before a peak for baseline (μs): 5000; period to search a decay time: 5000; fraction of peak to find a decay time: 0.5; period to average a baseline (μs): 2000; area threshold: 10; number of points to average for peak: 3; direction of peak: negative).

For evoked EPSC recording, pipettes were filled with a solution containing (in mM): 120 $CsMeSO_4$, 10 HEPES, 10 EGTA, 4 Na_2-ATP, 1 Na_3-GTP, 2 $MgCl_2$, 4 QX-314 (pH 7.32–7.36; osmolarity 294–298). AMPAR-EPSCs were recorded in whole-cell voltage-clamp mode at a holding potential of −70 mV using artificial cerebrospinal fluid containing 0.1 mM picrotoxin (Tocris, Cat# 1128 (2018)). Evoked synaptic currents were elicited by afferent fiber stimulation with a concentric bipolar electrode (FHC, Cat# 211386 (2018)) and controlled by a Model 2100 Isolated Pulse Stimulator (A-M Systems, Inc., RRID:SCR_016677). We gradually adjusted the stimulus intensity to ensure the maximum EPSC amplitude and to avoid the extra disturbance from eliciting multiple action potentials. Paired-pulse eEPSC ratios were recorded from the same hippocampal neurons at interpulse intervals of 50 ms (20 Hz), 100 ms (10 Hz), 200 ms (5 Hz), and 500 ms (2 Hz) (Hu et al., 2021; Regehr, 2012). Spontaneous EPSCs (sEPSCs) were recorded from the same hippocampal neurons 1 min after the paired-pulse stimulation.

2.6 | GST pull-down assay

The GST-Syt11 plasmid was constructed by inserting the cytosolic region (amino acids 37–428) of Syt11cDNA (AF000423) into the pGEX4T2 vector with a linker sequence of LVPRGSPGIP at its N-terminal. Proteins were induced by 0.2 µM IPTG at room temperature for 5 h and purified with GST Glutathione Sepharose^{TM} 4B beads (GE Healthcare, Cat# 17–0756–01 (2018)). Briefly, bacterial pellets from 200 ml LB culture medium were suspended in 10-ml lysis buffer (50 mM NaH$_2$PO$_4$, 300 mM NaCl, pH 8.0) containing 1 mg/ml lysozyme, 1×PI (protease inhibitor cocktail; Roche, Cat# 04693132001 (2018)), and 1 mM phenylmethylsulfonyl fluoride (PMSF). The cells were lysed for 30 min on ice and sonicated. Then, after centrifugation at 20 000 g for 15 min, the supernatant was incubated with 200-µl Glutathione Sepharose^{TM} 4B beads at 4°C for 5 h. After three washes in phosphate-buffered saline (PBS), the concentration of GST-tagged proteins immobilized on beads was quantified by Coomassie staining of SDS PAGE gels and the beads were stored at 4°C for further experiments.

Mice were anesthetized using isoflurane and rapidly decapitated. The brains were homogenized in lysis buffer (20 mM Tris (pH 7.5), 150 mM NaCl, 1% Triton X-100, 1 mM EDTA, 1×PI, and 1 mM PMSF) and rotated at 4°C for 2 h. After centrifugation for 15 min at 20 000 g at 4°C, 2 mg of total proteins was collected in the supernatant and pre-cleared for 1 h at 4°C with 20-µg Glutathione Sepharose^{TM} 4B beads. After a quick spin, the supernatant was incubated with 20 µg of immobilized GST fusion protein on Glutathione Sepharose^{TM} 4B beads at 4°C for 4 h. The resin was collected after a quick spin and underwent five washes with lysis buffer, followed by treatment with SDS sample buffer at 65°C for 10 min for western blotting.

2.7 | Co-immunoprecipitation

Co-IP was performed with 4-µg anti-vti1a antibody and its corresponding isotype IgG antibody. The mouse brain lysate (prepared in 20 mM Tris (pH 7.5), 500 mM NaCl, 1% Triton X-100, 1 mM EDTA, 1×PI, and 1 mM PMSF) was incubated with anti-vti1a antibody at 4°C overnight followed by 40-µl protein G Sepharose beads. After three washes with lysis buffer, the beads were treated with SDS sample buffer at 65°C for 10 min before western blotting.

2.8 | Purified protein-binding assays *in vitro*

The GST-Syt11 mutants contained the following amino-acid sequences: linker (37–156), Δlinker (157–428), C2A (157–290), ΔC2A (37–156 and 291–428), C2B (291–428), and ΔC2B (37–290). They were inserted into the pGEX4T2 vector the same as GST-Syt11.

The His-vti1a plasmid was constructed by inserting the cDNA of vti1a (NM_001293685.1) into the bacterial protein expression vector pET with a 6xHis tag at its N-terminal (pET-6xHis/mVti1a).

The bacterial pellets from 200-ml culture medium were suspended with 10 ml-lysis buffer (50 mM NaH$_2$PO4, 300 mM NaCl, pH 8.0) containing 1 mg/ml lysozyme, PI, and 1 mM PMSF. The cells were lysed for 30 min on ice and sonicated. To purify His-tag proteins, the centrifuged supernatant was incubated with 1-ml His-tag purification resin (Beyotime, Cat# P2218 [2019]) at 4°C for 1 h. The lysate was transferred to an Ni column, and washed three times with washing buffer (in mM: 50 NaH$_2$PO4, 300 NaCl, 2 imidazole, pH 8.0). The bound proteins were eluted with elution buffer (in mM: 50 NaH$_2$PO4, 300 NaCl, 50 imidazole, pH 8.0).

The binding essay was performed according to Yan et al., (2020) with modifications. Briefly, purified GST-Syt11 and mutants (immobilized on Glutathione Sepharose^{TM} 4B beads) were incubated with His-vti1a protein (2.5 µM) in 500 µl of reaction buffer (50 mM Tris-HCl, 100 mM NaCl, 0.5% Triton X-100, pH 8.0) at 4°C for 1 h. The bound fraction was washed five times with washing buffer (50 mM Tris-HCl, 150 mM NaCl, 0.5% Triton X-100, pH 8.0) and western blotting was performed.

2.9 | Immunofluorescence

Immunofluorescence experiments were performed as in Du et al., (2017). Briefly, neurons were fixed in 4% paraformaldehyde and quenched in 1 mg/ml NaBH$_4$ in TBS (in mM: 20 Tris pH 7.5, 154 NaCl, 2 EGTA, 2 MgCl$_2$). The cells were then blocked in TBS containing 2% bovine serum albumin and 0.02% saponin and treated sequentially with primary and secondary antibodies. The mounted cells were imaged under a Leica TCS SP8 confocal microscope with a 63× objective and 2.5× digital zoom. Co-localization was analyzed using the Pearson's coefficient plug-in in NIH ImageJ (RRID:SCR_003070).

2.10 | Western blotting

Western blotting experiments were performed as in Wang et al., (2016). In brief, cells were washed with PBS and suspended on ice in lysis buffer (20 mM Hepes, 100 mM KCl, 2 mM EDTA, 1% NP-40, 1 mM PMSF, and 1×PI, pH 7.4). After centrifugation at 15000 g for 15 min at 4°C, the supernatants were collected and boiled in SDS-PAGE buffer. Proteins were separated on 10% SDS-polyacrylamide gels and transferred to nitrocellulose filter membranes. Each membrane was blocked for 1 h in PBS containing 0.1% Tween 20 (v/v) and 5% non-fat dry milk (w/v). After washing three times with 0.1% Tween 20 containing PBS (PBST), the blots were incubated with primary antibodies at 4°C overnight in PBST containing 2% bovine serum albumin and secondary antibodies at room temperature for 1 h. Blots were scanned with an Odyssey infrared imaging system (LI-COR Biosciences, RRID:SCR_014579) and quantified with ImageJ.

2.11 | Statistical analysis

All experiments were independently replicated at least three times. Data are shown as the mean ± SEM. Results were analyzed using

GraphPad Prism 7.0 software (RRID: SCR_002798). The coefficient of variation was calculated as $SD_{eEPSC}/Mean_{eEPSC}$ (Kullmann, 1994). Statistical comparisons were made with the two-tailed unpaired *t*-test, one-way ANOVA, two-way ANOVA, or the Kolmogorov–Smirnov test as indicated. Differences with $p < 0.05$ were accepted as significant. No statistical method was used to predetermine sample sizes, but our sample sizes are similar to those generally used in the field. The normal distribution of the data was assessed by the Kolmogorov–Smirnov test. No test for outliers was applied. No data were excluded.

3 | RESULTS

3.1 | Synaptotagmin-11 inhibits spontaneous neurotransmission

To investigate the function of Syt11 in spontaneous release, we used Syt11 knockout (KO) hippocampal neurons. Primary cultured hippocampal neurons from floxed Syt11 knock-in mice were infected with cre-expressing lentivirus to generate Syt11-KO neurons, while catalytically inactive Δcre served as a negative control. This applies
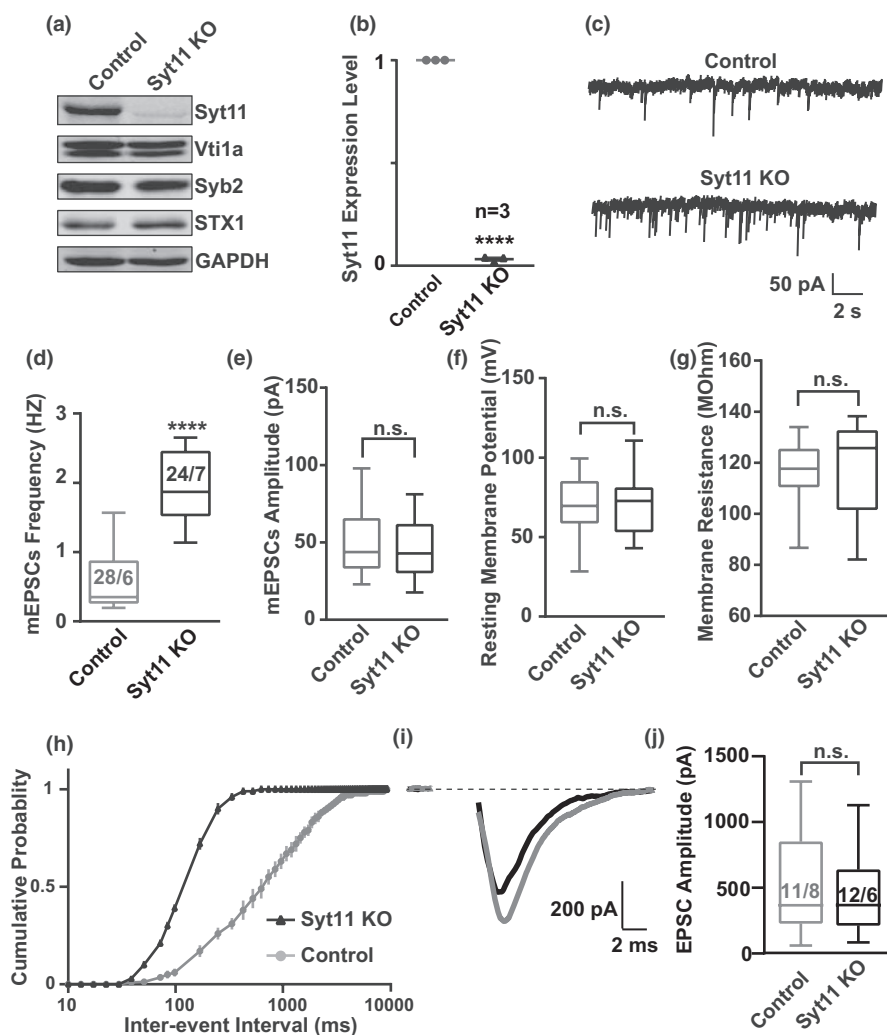

FIGURE 1 Knockout of Syt11 enhances spontaneous neurotransmission. (a and b) Representative western blots (a) and quantification (b) of Syt11 protein expression levels in primary cultured hippocampal control neurons (Δcre) and Syt11-KO neurons (cre) (*n* = 3 independent cell culture preparations; error bars represent mean ± SEM; ****$p < 0.0001$, Student's *t*-test). (c and d) Representative traces of mEPSCs (c) and average frequency (d) of control (0.55 ± 0.07 Hz, *n* = 28 cells/6 independent cell culture preparations) and Syt11-KO neurons (1.94 ± 0.09 Hz, *n* = 24 cells/7 independent cell culture preparations) (mean ± SEM; ****$p < 0.0001$). (e–g) Average amplitude (e) (50.19 ± 3.73 vs. 45.89 ± 3.60 pA), resting membrane potential (f) (70.12 ± 3.42 vs. 70.35 ± 3.65 mV), and membrane resistance (g) (116.20 ± 2.10 vs. 119.10 ± 3.42 MΩ) of control and Syt11-KO neurons (mean ± SEM; n.s., not significant). (h) Average cumulative probability plot of mEPSC inter-event intervals of control and Syt11-KO neurons as in (d). Syt11 KO increased the high-frequency events ($p < 0.0001$, Kolmogorov–Smirnov test). (i and j) Representative traces of eEPSCs (i) and average amplitude (j) of control (533.88 ± 133.03 pA, *n* = 11 cells/8 independent cell culture preparations) and Syt11-KO neurons (443.19 ± 87.07 pA, *n* = 12 cells/6 independent cell culture preparations) (mean ± SEM; n.s., not significant). The coefficient of variation for eEPSC amplitudes of control neurons is 0.28 ± 0.05, and that of Syt11-KO neurons is 0.22 ± 0.03. Both the eEPSC amplitudes and coefficients of variation show no significant difference in control and Syt11-KO neurons

to all the KO experiments described here. The KO efficiency of Syt11 was >98%, while SNARE proteins involved in spontaneous release—syb2, vti1a, and syntaxin1—remained unaffected (Figure 1a,b). Next, we monitored the mEPSCs in the presence of TTX and the GABA$_A$ receptor blocker bicuculline in control and Syt11-KO neurons. The Syt11-KO neurons showed an increased average frequency of spontaneous release by ~4-fold (Figure 1c,d). On the other hand, the mEPSC amplitudes did not change significantly (Figure 1e), consistent with a previous report (Shimojo et al., 2019). The membrane properties of Syt11-KO neurons did not differ from controls, since the resting membrane potential and membrane resistance did not significantly differ (Figure 1f,g). Interestingly, Syt11-KO greatly enhanced the high-frequency spontaneous neurotransmission that occurred at lower inter-event intervals (Figure 1h). The amplitudes of evoked EPSCs (eEPSCs) and coefficient of variation in Syt-11 KO neurons did not significantly differ from controls (Figure 1i,j), which supports a selective action of Syt11 in regulating spontaneous release.

When we over-expressed Syt11 by infecting hippocampal neurons with lentivirus expressing Syt11 (Figure 2a,b), we found a significant decrease of mEPSC frequency (Figure 2c,d). The over-expression (OE) level of Syt11 protein was ~1.7-fold that of endogenous expression. Under this condition, the mEPSC amplitudes and membrane properties were not affected (Figure 2e–g). All together, these results showed that Syt11 suppresses spontaneous release under physiological conditions.

3.2 | Syt11 directly interacts with vti1a

To understand the molecular mechanism of Syt11 inhibition in spontaneous transmission, we searched for its interacting proteins using GST-Syt11 in pull-down experiments in mouse brain extracts (Figure 3a). We found that vti1a was specifically pulled down by Syt11, while syb2 and syntaxin1 failed to bind Syt11. Furthermore, co-immunoprecipitation experiments with vti1a antibody showed that Syt11 was in the same complex with vti1a (Figure 3b). To test whether Syt11 binds vti1a directly, we purified His-tagged vti1a and incubated it with purified GST-Syt11 (Figure 3c). The result showed that Syt11 directly interacted with vti1a (Figure 3d).
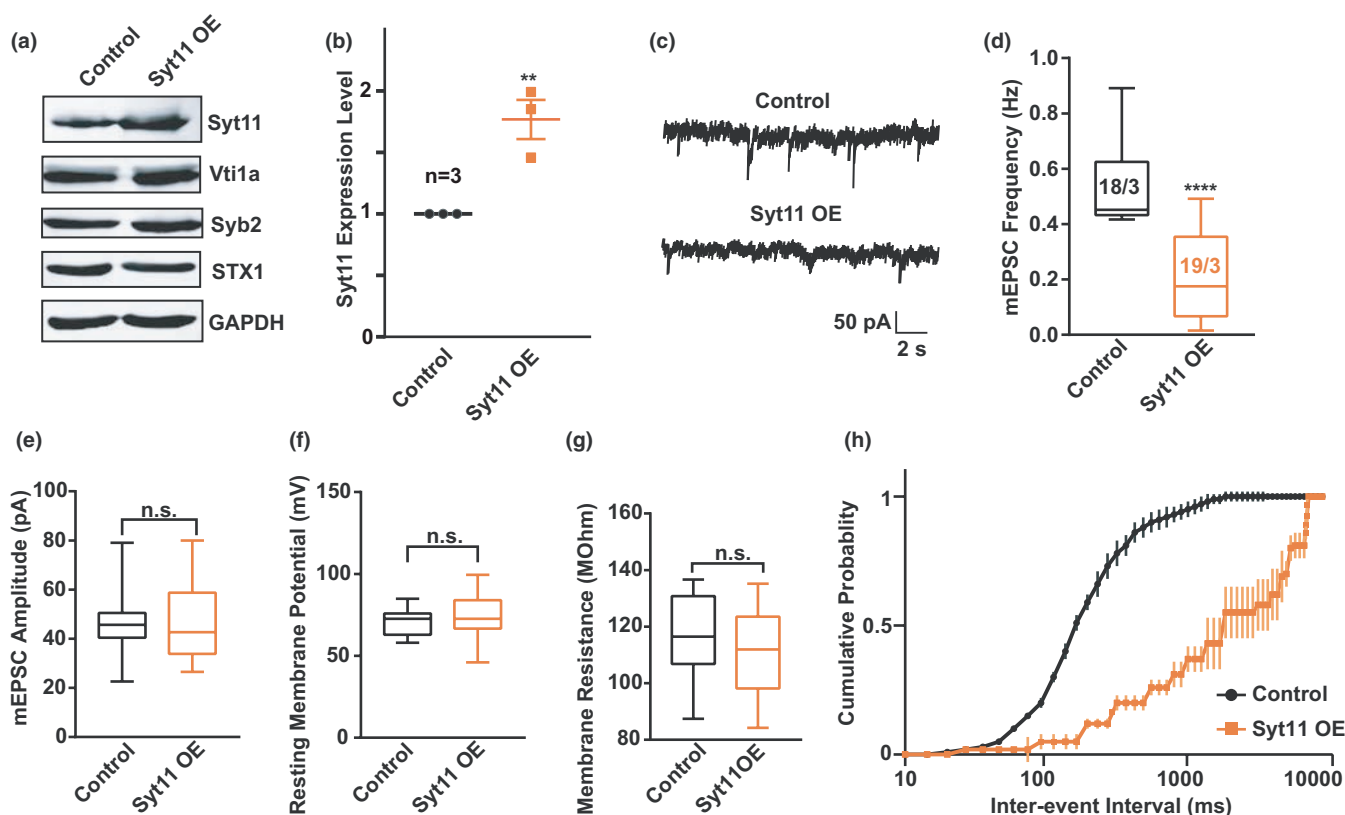

FIGURE 2 Over-expression of Syt11 decreases spontaneous neurotransmission. (a and b) Representative western blots (a) and quantification (b) of Syt11 protein expression levels in primary cultured hippocampal control neurons (GFP) and Syt11-OE neurons ($n = 3$ independent cell culture preparations; error bars represent mean ± SEM; **$p < 0.01$, Student's t-test). (c and d) Representative mEPSC traces (c) and average frequency (d) of control (0.54 ± 0.04 Hz, $n = 18$ cells/3 independent cell culture preparations) and Syt11-OE neurons (0.21 ± 0.03 Hz, $n = 19$ cells/3 independent cell culture preparations) (mean ± SEM; ****$p < 0.0001$). (e–g) Average amplitude (e) (47.10 ± 3.08 vs. 46.39 ± 3.62 pA), resting membrane potential (f) (71.12 ± 1.74 vs. 73.75 ± 2.93 mV), and membrane resistance (g) (115.10 ± 3.64 vs. 111.10 ± 3.70 MΩ) of control and Syt11-OE neurons (mean ± SEM; n.s., not significant). (h) Average cumulative probability of mEPSC inter-event intervals of control and Syt11-OE neurons as in (d). Syt11 OE decreased the high-frequency events ($p < 0.0001$, Kolmogorov–Smirnov test)
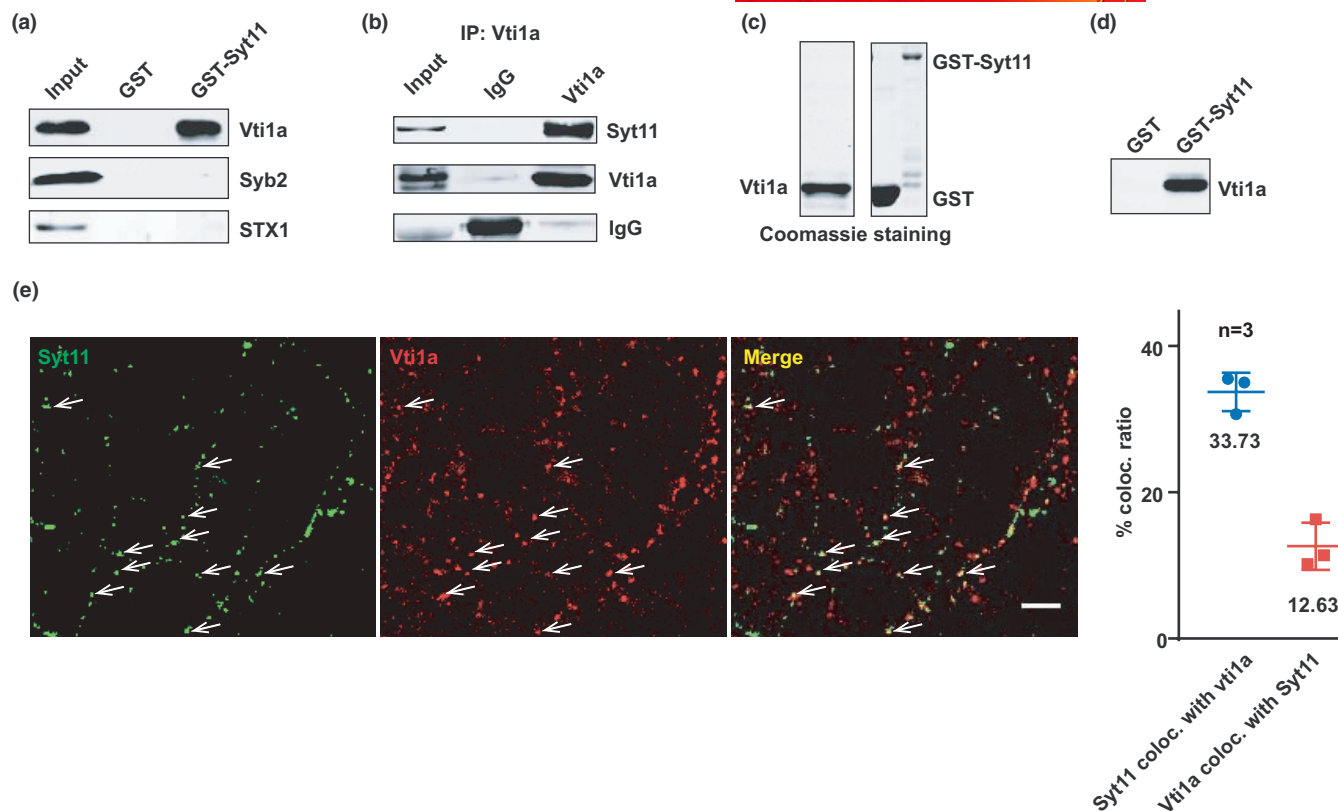
FIGURE 3 Syt11 directly interacts with vti1a. (a) Western blots of GST pull-down experiments. Purified recombinant GST-Syt11 protein was incubated with mouse brain extract and bound proteins were detected with anti-vti1a, anti-Syb2, and anti-syntaxin1 antibodies ($n = 3$ independent cell culture preparations). (b) Western blots of co-immunoprecipitation of mouse anti-vti1a antibody with Syt11, while Syb2 and syntaxin1 were absent. Two percent of the mouse brain extract was loaded as input ($n = 3$ independent cell culture preparations). (c) SDS gels showing purified GST-Syt11 and GST visualized by Coomassie brilliant blue staining ($n = 3$ independent cell culture preparations). (d) GST pull-down with purified GST-Syt11 and His-vti1a ($n = 3$ independent cell culture preparations). (e) Confocal images showing hippocampal neurons expressing Myc-Syt11 stained with antibodies against Myc (green) and vti1a (red). Arrows indicate co-localized puncta at synapses ($n = 3$ independent cell culture preparations). Scale bar, 10 μm

To explore whether the Syt11-vti1a interaction occurs at synapses, we performed immunofluorescence experiments in hippocampal neurons expressing myc-Syt11 (Figure 3e). Syt11 was partially co-localized with endogenous vti1a in boutons, supporting its diverse functions in synaptic exocytosis and endocytosis (Wang et al., 2016).

3.3 | Syt11 inhibits spontaneous neurotransmission *via* vti1a

Since Syt11 specifically bound vti1a, which selectively functions in spontaneous release (Ramirez et al., 2012), we reasoned that Syt11 may regulate spontaneous neurotransmission by inhibiting vti1a. To test this hypothesis, we knocked down vti1a in Syt11-KO hippocampal neurons (Figure 4a,b). If vti1a is the main target of Syt11 regulation, knocking down vti1a should eliminate the increased frequency in Syt11-KO cells. Two different lentivirus-expressing shRNAs against vti1a both reduced its protein expression to ~50%, while a non-targeting shRNA served as the negative control. Indeed,

vti1a knockdown (KD) by both shRNAs reversed the Syt11-KO phenotype by decreasing the frequency of mEPSCs, in particular the high-frequency events (Figure 4c–e). We also confirmed that vti1a-KD itself reduced the spontaneous release frequency, especially high-frequency events (Ramirez et al., 2012). Syt11-KO and vti1a-KD showed an average frequency and cumulative probability similar to vti1a-KD alone, indicating that vti1a is the main target of Syt11 regulation.

To validate that Syt11-vti1a selectively functions in spontaneous release, we monitored eEPSCs and sEPSCs (without TTX) from the same neurons (Figure 5). Paired-pulse stimulation at 50 ms (20 Hz), 100 ms (10 Hz), 200 ms (5 Hz), and 500 ms (2 Hz) intervals showed that paired-pulse ratios were unaffected in the absence of Syt11 and/or vti1a (Figure 5a,b), suggesting that Syt11 and vti1a do not function in evoked release. On the other hand, sEPSCs recorded from the same cells after paired-pulse stimulation showed similar phenotypes as the mEPSCs (Figure 5c, d vs. Figure 4c,d). Syt11-KO significantly increased sEPSC frequency while vti1a-KD reversed the Syt11-KO phenotype. These results support the hypothesis that Syt11-vti1a specifically modulates spontaneous release.
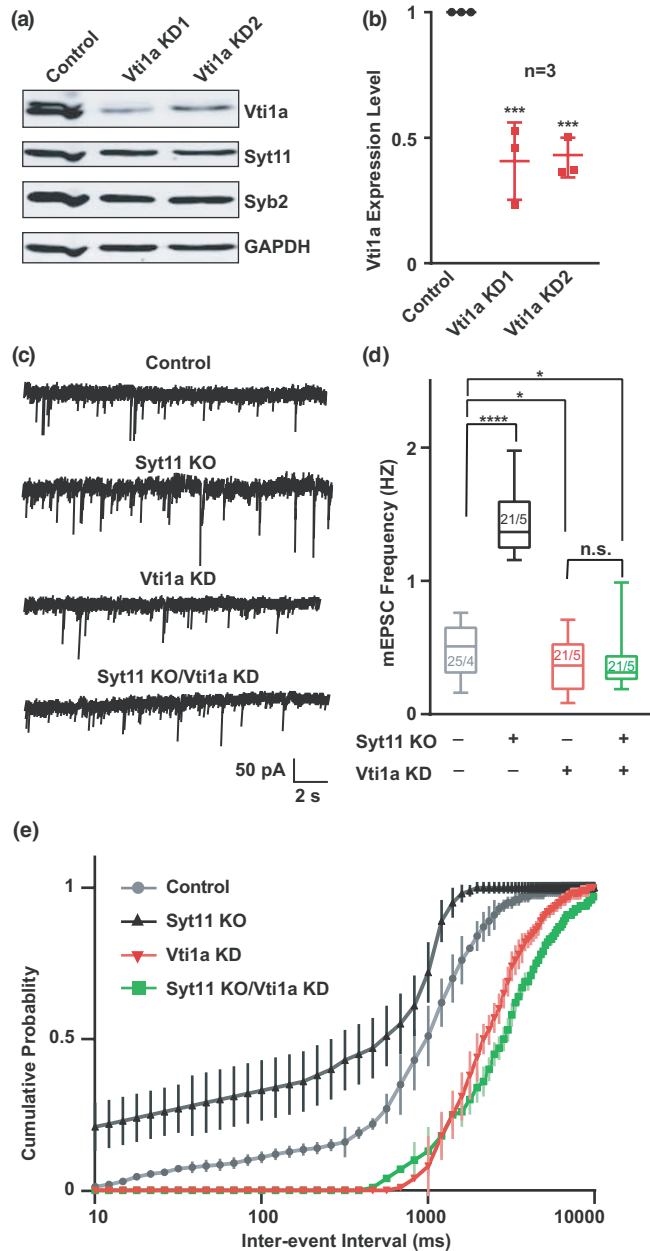
FIGURE 4 Syt11 inhibits spontaneous neurotransmission *via* vti1a. (a and b) Representative western blots (a) and quantification (b) of vti1a protein expression levels in primary cultured hippocampal neurons infected with control (non-targeting shRNA, NT), vti1a KD-1, and vti1a KD-2 lentivirus ($n = 3$ independent cell culture preparations; error bars represent mean ± SEM; ***$p < 0.001$, one-way ANOVA. (c and d) Representative traces of mEPSCs (c) and average frequency (d) in control (Δcre + NT) (0.49 ± 0.04 Hz, $n = 25$ cells/4 independent cell culture preparations), Syt11-KO (cre +NT) (1.44 ± 0.05 Hz, $n = 21$ cells/5 independent cell culture preparations), vti1a-KD (Δcre + KD1 or KD2) (0.37 ± 0.04 Hz, $n = 21$ cells/5 independent cell culture preparations), and Syt11-KO/vti1a-KD (cre +KD1 or KD2) (0.38 ± 0.04 Hz, $n = 21$ cells/5 independent cell culture preparations) neurons (mean ± SEM; ****$p < 0.0001$, *$p < 0.05$, two-way ANOVA). (e) Average cumulative probability of mEPSC inter-event intervals of control, Syt11-KO, vti1a-KD, and Syt11-KO/vti1a-KD neurons as in (d). Both vti1a-KD and Syt11-KO/vti1a-KD have fewer high-frequency events than controls (vti1a KD $p = 0.0001$, Syt11-KO/vti1a-KD $p < 0.0001$, Kolmogorov–Smirnov test)

3.4 | Syt11 interacts with vti1a through multiple domains

To identify the domains required for Syt11 binding to vti1a, we constructed a series of Syt11 truncation mutants that included its cytosolic domain (GST-Syt11), the cytosolic domain without the linker, C2A, or C2B domain (GST-ΔLinker, GST-ΔC2A, GST-ΔC2B), and the linker, C2A, and C2B domains alone (GST-Linker, GST-C2A, GST-C2B, Figure 6a). Coomassie staining revealed the purity of these mutants and those that included the linker region were more vulnerable to degradation (Figure 6b). All these mutants bound vti1a to different extents. Among them, ΔC2A displayed weaker binding than ΔC2B or ΔLinker, while the C2A domain showed stronger interaction than the C2B or Linker domain (Figure 6c). These results revealed an important role of the C2A domain in the Syt11–vti1a interaction, consistent with a previous report in which the C2A domain of Syt11 was shown to bind vti1a more strongly than C2B (Milochau et al., 2014).

3.5 | C2A domain rescues Syt11-KO phenotype

Since the C2A domain of Syt11 had a high binding affinity for vti1a and vti1a was the main target of the Syt11 regulation of spontaneous release, we tested whether the C2A domain by itself rescued the Syt11-KO phenotype similar to the full-length (FL) protein. Lentivirus expressing Syt11 FL or Syt11 C2A was used in KO neurons while GFP was used as the negative control (Figure 7a,b). As expected, Syt11-KO increased the frequency of mEPSCs and both Syt11 FL and Syt11 C2A expressions largely rescued the phenotype both in average frequency and cumulative probability (Figure 7a–c). Therefore, the C2A domain of Syt11 was sufficient to reverse the KO phenotype. As no other binding proteins have been reported for the C2A domain of Syt11 (Milochau et al., 2014), these results further supported our hypothesis that Syt11 inhibits spontaneous neurotransmission mainly through its interaction with vti1a.

4 | DISCUSSION

In this study, we identified Syt11 as a novel inhibitor of spontaneous neurotransmission through its direct binding with vti1a. Knockout of endogenous Syt11 in hippocampal neurons increased the frequency of spontaneous release events while over-expression suppressed it (Figures 1 and 2). The specific interaction of Syt11 with vti1a was revealed by GST pull-down, co-immunoprecipitation, purified protein binding assays, and co-localization experiments (Figure 3). Importantly, the increased spontaneous release in Syt11-KO neurons was reversed by vti1a KD, identifying vti1a as the main target of Syt11 inhibition (Figure 4). Furthermore, we showed that Syt11 directly bound to vti1a through its C2A domain (Figure 6). Expression of the full-length Syt11 protein or the C2A domain alone both rescued the Syt11-KO phenotype, further supporting the
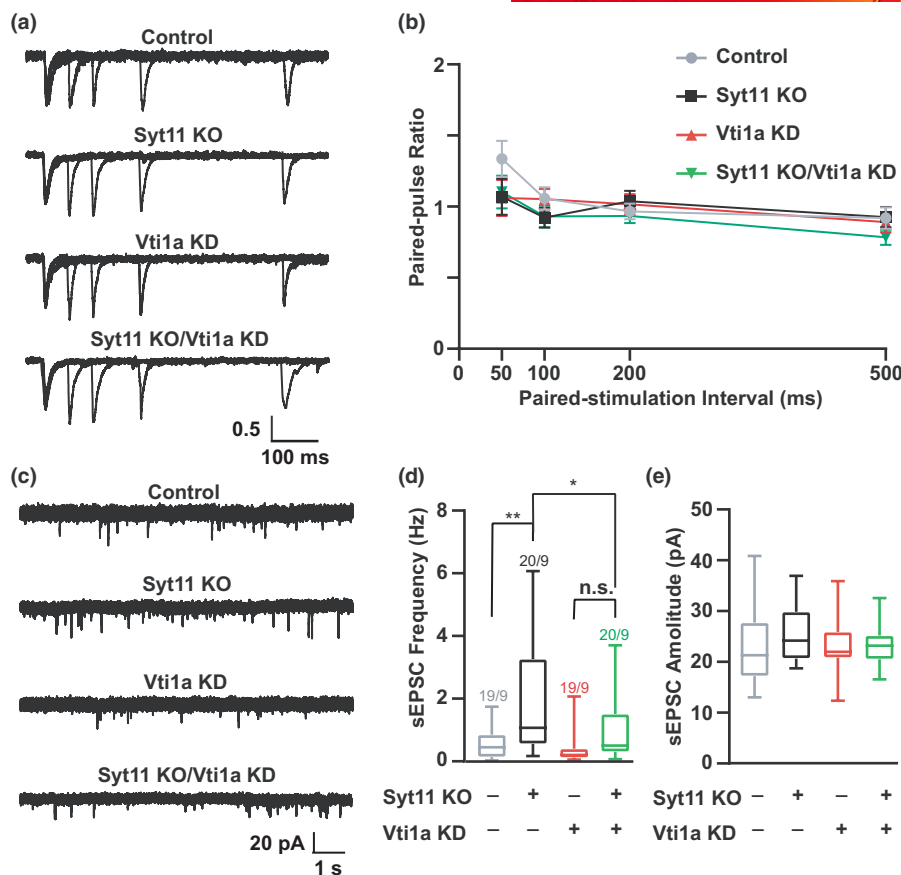
FIGURE 5 Syt11 does not affect evoked neurotransmission. (a and c) Representative eEPSC and sEPSC traces from the same cells (a). (b) Paired-pulse ratios in control (1.34 ± 0.13, n = 19 cells/9 independent cell culture preparations; 1.06 ± 0.08, n = 23 cells/9 independent cell culture preparations; 0.97 ± 0.05, n = 26 cells/9 independent cell culture preparations; 0.92 ± 0.07, n = 21 cells/9 independent cell culture preparations), Syt11-KO (1.07 ± 0.13, n = 19 cells/9 independent cell culture preparations; 0.92 ± 0.07, n = 20 cells/9 independent cell culture preparations; 1.04 ± 0.07, n = 24 cells/9 independent cell culture preparations; 0.95 ± 0.07, n= 19 cells/9 independent cell culture preparations), vti1a-KD (1.06 ± 0.13, n = 19 cells/9 independent cell culture preparations; 1.05 ± 0.07, n = 18 cells/9 independent cell culture preparations, 1.02 ± 0.07, n=24 cells/9 independent cell culture preparations; 0.89 ± 0.07, n = 18 cells/9 independent cell culture preparations), and Syt11-KO/vti1a-KD (1.10 ± 0.11, n = 26 cells/9 independent cell culture preparations; 0.93 ± 0.08, n = 22 cells/9 independent cell culture preparations; 0.93 ± 0.05, n = 30 cells/9 independent cell culture preparations; 0.78 ± 0.05, n = 20 cells/9 independent cell culture preparations) neurons at 50 ms, 100 ms, 200 ms, and 500 ms paired-stimulation, respectively (mean ± SEM; two-way ANOVA). (d) Average sEPSC frequency in control (0.56 ± 0.10 Hz, n = 19 cells/9 independent cell culture preparations), Syt11-KO (1.70 ± 0.38 Hz, n = 20 cells/9 independent cell culture preparations), vti1a-KD (0.41 ± 0.13 Hz, n = 19 cells/9 independent cell culture preparations), and Syt11-KO/vti1a-KD (0.92 ± 0.21 Hz, n = 20 cells/9 independent cell culture preparations) neurons (mean ± SEM; **p < 0.01, *p < 0.05, two-way ANOVA). (e) Average sEPSC amplitude in control (23.00 ± 1.80 pA, n = 19 cells/9 independent cell culture preparations), Syt11-KO (25.65 ± 1.21 pA, n = 20 cells/9 independent cell culture preparations), vti1a-KD (23.11 ± 1.16 pA, n = 19 cells/9 independent cell culture preparations), and Syt11-KO/vti1a-KD (22.80 ± 0.81 pA, n = 20 cells/9 independent cell culture preparations) neurons (mean ± SEM; two-way ANOVA). Paired-pulse ratios are unaffected in the absence of Syt11 and/or vti1a while sEPSCs are affected similar to mEPSCs

hypothesis that Syt11 inhibits spontaneous neurotransmission *via* vti1a (Figure 7).

Vti1a-containing vesicles are actively trafficked at rest and support spontaneous neurotransmission (Ramirez et al., 2012). We showed here that Syt11 selectively regulated vti1a-mediated spontaneous release since vti1a KD abolished the Syt11-KO phenotype and Syt11 interacted with vti1a, but not syb2. In Syt11-KO terminals, the frequency of mEPSCs increased ~4-fold. As both syb2- and vti1a-vesicles contributed to spontaneous neurotransmission, this result suggested that the majority of vti1a-containing vesicles

(>75%) are "clamped" under physiological conditions. Strikingly, Syt11-OE (at ~1.7-fold of the endogenous level) reduced mEPSC frequency to ~1/3 of control. If we assume that all vti1a-vesicles are clamped under this condition, these data suggest that vti1a-vesicles contribute to ~2/3 of spontaneous release. It is possible that a compensation mechanism occurred in cultured hippocampal neurons during the time of Syt11-KO or the over-expression process, which lasted for 10–11 days. It remains to be determined whether acute manipulation of Syt11 protein levels leads to even more severe phenotypes. Altogether, our results point to a crucial role of vti1a in
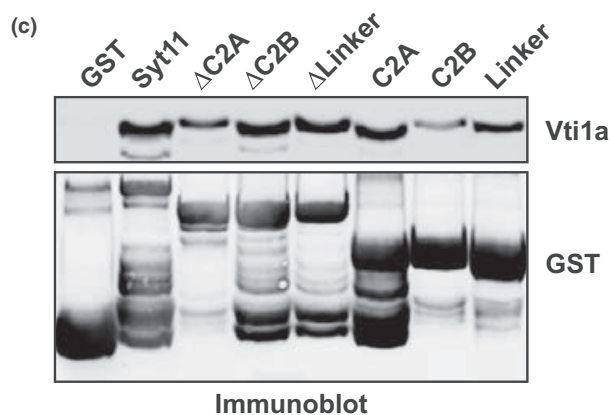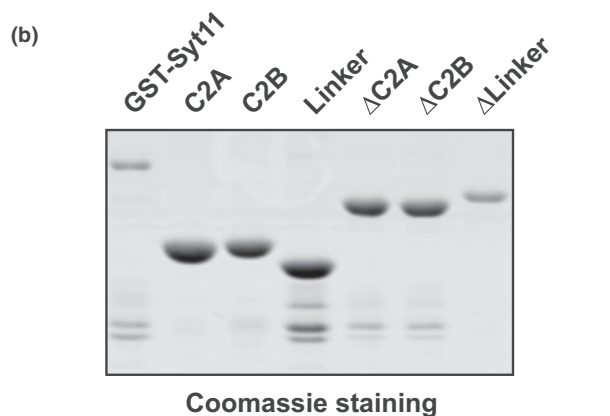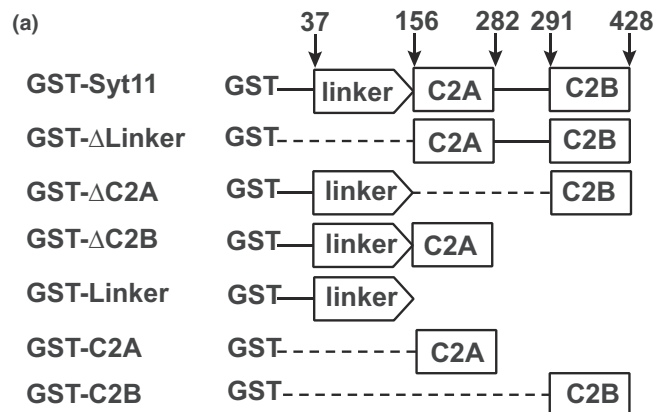
(a)

(b)

Coomassie staining

(c)

Immunoblot

FIGURE 6 Syt11 interacts with vti1a through multiple domains. (a) Schematic of GST-Syt11 and GST-Syt11 truncations (solid lines, amino acids included; dashed lines, deletions). (b) Purified GST-Syt11 and its mutants visualized by Coomassie brilliant blue staining of SDS gels ($n = 4$ independent cell culture preparations). (c) Western blots of GST pull-down with purified GST-Syt11, its mutations, and His-vti1a ($n = 4$ independent cell culture preparations)

(a)

(b)

(c)

FIGURE 7 The C2A domain rescues the Syt11-KO phenotype. (a and b) Representative mEPSC traces (a) and average frequency (b) of control (Δcre + GFP) (0.53 ± 0.04 Hz, $n = 25$ cells/5 independent cell culture preparations), Syt11-KO (cre + GFP) (2.02 ± 0.12 Hz, $n = 26$ cells/5 independent cell culture preparations), and Syt11-KO neurons infected with Syt11 FL (0.81 ± 0.05 Hz, $n = 26$ cells/6 independent cell culture preparations) or Syt11 C2A lentivirus (0.77 ± 0.05 Hz, $n = 21$ cells/5 independent cell culture preparations) (mean $\pm$ SEM; ****$p < 0.0001$, one-way ANOVA). (c) Average cumulative probability of mEPSC inter-event intervals in control, Syt11-KO, and Syt11-KO neurons infected with Syt11 FL or Syt11 C2A as in (b). Both Syt11 FL and Syt11 C2A significantly reverse the Syt11 KO phenotype (Syt11 FL $p < 0.0001$, Syt11 C2A $p < 0.0001$, Kolmogorov–Smirnov test)

spontaneous neurotransmission and its precise regulation by Syt11 under physiological conditions. It would be interesting to investigate whether abnormal regulation of vti1a by Syt11 participates in brain diseases, such as schizophrenia and Parkinson's disease, in which over-expression of Syt11 has been suggested (Huynh et al., 2003; Inoue et al., 2007; Wang et al., 2018). Given the diverse functions
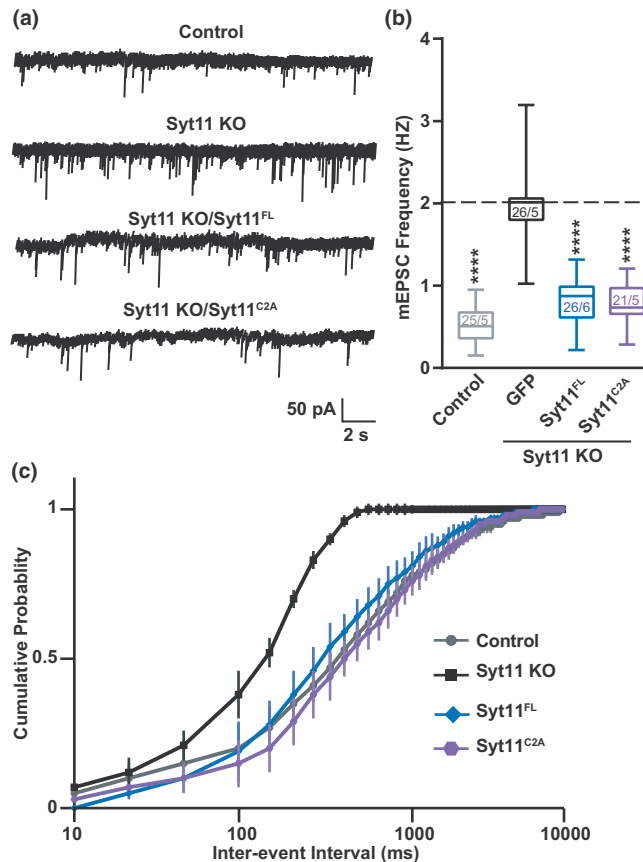
of vti1a in both spontaneous and evoked neurotransmission, as well as dense-core vesicle secretion (Crawford et al., 2017; Emperador-Melero et al., 2018, 2019; Kononenko & Haucke, 2012; Ramirez et al., 2012; Walter et al., 2014), a pathological expression level of Syt11 may lead to wide-ranging defects in cell-to-cell communication in the brain through the Syt11–vti1a interaction.

To date, vti1a is the only interactor identified for the C2A domain of Syt11 (Milochau et al., 2014). Its C2A domain also fails to bind phospholipids biochemically (von Poser et al., 1997). On the contrary, the C2A domain of Syt1 binds the SNARE complex and phospholipids in a Ca^{2+}-dependent manner (Pallanck, 2003). The C2A domain of Syt4 shows 73% identity and 87% similarity with Syt11, while that of Syt1 shows 49% identity and 66% similarity. Syt4 regulates evoked and spontaneous neurotransmission similar to Syt11

(Dean et al., 2009). It is possible that Syt4, and perhaps other Syt members, also inhibits vti1a under resting conditions. Further studies are needed to map the binding site on the C2A domain of Syt11 and to understand whether vti1a is regulated by other Syt members and/or proteins. As the important roles of spontaneous neurotransmission are increasingly being revealed, it would be interesting to explore the regulation of molecularly distinct vesicles responsible for spontaneous release.

ACKNOWLEDGMENTS

CONFLICT OF INTEREST

The authors declare no conflict of interest.

AUTHOR CONTRIBUTIONS

CXZ, RL, and SZ conceived and designed the study, WRL, YLW, CL, PG, FFZ, and JCL performed experiments, WRL, YLW, and CL analyzed data, MH and SZ interpreted data, CXZ, WRL, and SZ wrote the manuscript.

DATA AVAILABILITY STATEMENT

Data sharing is not applicable as all data are included in this article.

ORCID

Claire Xi Zhang https://orcid.org/0000-0002-4687-039X

REFERENCES

Advani, R. J., Bae, H. R., Bock, J. B., Chao, D. S., Doung, Y. C., Prekeris, R., Yoo, J. S., & Scheller, R. H. (1998). Seven novel mammalian SNARE proteins localize to distinct membrane compartments. *Journal of Biological Chemistry*, 273, 10317–10324. https://doi.org/10.1074/jbc.273.17.10317

Andreae, L. C., & Burrone, J. (2018). The role of spontaneous neurotransmission in synapse and circuit development. *Journal of Neuroscience Research*, 96, 354–359. https://doi.org/10.1002/jnr.24154

Antonin, W., Fasshauer, D., Becker, S., Jahn, R., & Schneider, T. R. (2002). Crystal structure of the endosomal SNARE complex reveals common structural principles of all SNAREs. *Natural Structural Biology*, 9, 107–111. https://doi.org/10.1038/nsb746

Bacaj, T., Wu, D., Yang, X., Morishita, W., Zhou, P., Xu, W., Malenka, R. C., & Sudhof, T. C. (2013). Synaptotagmin-1 and synaptotagmin-7 trigger synchronous and asynchronous phases of neurotransmitter release. *Neuron*, 80, 947–959. https://doi.org/10.1016/j.neuron.2013.10.026

Bal, M., Leitz, J., Reese, A. L., Ramirez, D. M., Durakoglugil, M., Herz, J., Monteggia, L. M., & Kavalali, E. T. (2013). Reelin mobilizes a VAMP7-dependent synaptic vesicle pool and selectively augments spontaneous neurotransmission. *Neuron*, 80, 934–946. https://doi.org/10.1016/j.neuron.2013.08.024

Bento, C. F., Ashkenazi, A., Jimenez-Sanchez, M., & Rubinsztein, D. C. (2016). The Parkinson's disease-associated genes ATP13A2 and SYT11 regulate autophagy via a common pathway. *Nature Communications*, 7, 11803. https://doi.org/10.1038/ncomms11803

Cornelisse, L. N., Tsivtsivadze, E., Meijer, M., Dijkstra, T. M., Heskes, T., & Verhage, M. (2012). Molecular machines in the synapse: overlapping protein sets control distinct steps in neurosecretion. *PLoS Computational Biology*, 8, e1002450. https://doi.org/10.1371/journal.pcbi.1002450

Crawford, D. C., Ramirez, D. M., Trauterman, B., Monteggia, L. M., & Kavalali, E. T. (2017). Selective molecular impairment of spontaneous neurotransmission modulates synaptic efficacy. *Nature Communications*, 8, 14436. https://doi.org/10.1038/ncomms14436

Dean, C., Liu, H., Dunning, F. M., Chang, P. Y., Jackson, M. B., & Chapman, E. R. (2009). Synaptotagmin-IV modulates synaptic function and long-term potentiation by regulating BDNF release. *Nature Neuroscience*, 12, 767–776. https://doi.org/10.1038/nn.2315

Du, C., Wang, Y., Zhang, F., Yan, S., Guan, Y., Gong, X., Zhang, T., Cui, X., Wang, X., & Zhang, C. X. (2017). Synaptotagmin-11 inhibits cytokine secretion and phagocytosis in microglia. *Glia*, 65, 1656–1667. https://doi.org/10.1002/glia.23186

Emperador-Melero, J., Huson, V., van Weering, J., Bollmann, C., Fischer von Mollard, G., Toonen, R. F., & Verhage, M. (2018). Vti1a/b regulate synaptic vesicle and dense core vesicle secretion via protein sorting at the Golgi. *Nature Communications*, 9, 3421. https://doi.org/10.1038/s41467-018-05699-z

Emperador-Melero, J., Toonen, R. F., & Verhage, M. (2019). Vti proteins: Beyond endolysosomal trafficking. *Neuroscience*, 420, 32–40. https://doi.org/10.1016/j.neuroscience.2018.11.014.

Fatt, P., & Katz, B. (1950). Some observations on biological noise. *Nature*, 166, 597–598. https://doi.org/10.1038/166597a0

Fatt, P., & Katz, B. (1952). Spontaneous subthreshold activity at motor nerve endings. *Journal of Physiology*, 117, 109–128.

Fawley, J. A., Hofmann, M. E., & Andresen, M. C. (2014). Cannabinoid 1 and transient receptor potential vanilloid 1 receptors discretely modulate evoked glutamate separately from spontaneous glutamate transmission. *Journal of Neuroscience*, 34, 8324–8332. https://doi.org/10.1523/JNEUROSCI.0315-14.2014

Fredj, N. B., & Burrone, J. (2009). A resting pool of vesicles is responsible for spontaneous vesicle fusion at the synapse. *Nature Neuroscience*, 12, 751–758. https://doi.org/10.1038/nn.2317

Geppert, M., Goda, Y., Hammer, R. E., Li, C., Rosahl, T. W., Stevens, C. F., & Sudhof, T. C. (1994). Synaptotagmin I: a major Ca^{2+} sensor for transmitter release at a central synapse. *Cell*, 79, 717–727. https://doi.org/10.1016/0092-8674(94)90556-8

Glitsch, M. (2006). Selective inhibition of spontaneous but not Ca^{2+}-dependent release machinery by presynaptic group II mGluRs in rat cerebellar slices. *Journal of Neurophysiology*, 96, 86–96.

Gonzalez-Islas, C., Bulow, P., & Wenner, P. (2018). Regulation of synaptic scaling by action potential-independent miniature neurotransmission. *Journal of Neuroscience Research*, 96, 348–353. https://doi.org/10.1002/jnr.24138

Groemer, T. W., & Klingauf, J. (2007). Synaptic vesicles recycling spontaneously and during activity belong to the same vesicle pool. *Nature Neuroscience*, 10, 145–147. https://doi.org/10.1038/nn1831

Groffen, A. J., Martens, S., Arazola, R. D., Cornelisse, L. N., Lozovaya, N., de Jong, A. P., Goriounova, N. A., Habets, R. L., Takai, Y., Borst, J. G., & Brose, N. (2010). Doc2b is a high-affinity Ca^{2+} sensor for spontaneous neurotransmitter release. *Science*, 327, 1614–1618.

Hu, H., Wang, X., Li, C., Li, Y., Hao, J., Zhou, Y., Yang, X., Chen, P., Shen, X., & Zhang, S. (2021). Loss of Dysbindin implicates synaptic vesicle

replenishment dysregulation as a potential pathogenic mechanism in schizophrenia. *Neuroscience*, 452, 138–152. https://doi.org/10.1016/j.neuroscience.2020.10.020

Hua, Z., Leal-Ortiz, S., Foss, S. M., Waites, C. L., Garner, C. C., Voglmaier, S. M., & Edwards, R. H. (2011). v-SNARE composition distinguishes synaptic vesicle pools. *Neuron*, 71, 474–487. https://doi.org/10.1016/j.neuron.2011.06.010

Huntwork, S., & Littleton, J. T. (2007). A complexin fusion clamp regulates spontaneous neurotransmitter release and synaptic growth. *Nature Neuroscience*, 10, 1235–1237. https://doi.org/10.1038/nn1980

Huynh, D. P., Scoles, D. R., Nguyen, D., & Pulst, S. M. (2003). The autosomal recessive juvenile Parkinson disease gene product, parkin, interacts with and ubiquitinates synaptotagmin XI. *Human Molecular Genetics*, 12, 2587–2597. https://doi.org/10.1093/hmg/ddg269

Ikeda, K., & Bekkers, J. M. (2009). Counting the number of releasable synaptic vesicles in a presynaptic terminal. *Proceedings of the National Academy of Sciences*, 106, 2945–2950. https://doi.org/10.1073/pnas.0811017106

Inoue, S., Imamura, A., Okazaki, Y., Yokota, H., Arai, M., Hayashi, N., Furukawa, A., Itokawa, M., & Oishi, M. (2007). Synaptotagmin XI as a candidate gene for susceptibility to schizophrenia. *American Journal of Medical Genetics. Part B, Neuropsychiatric Genetics: The Official Publication of the International Society of Psychiatric Genetics*, 144B, 332–340. https://doi.org/10.1002/ajmg.b.30465

International Parkinson Disease Genomics Consortium, Nalls, M. A., Plagnol, V., Hernandez, D. G., Sharma, M., Sheerin, U.-M., Saad, M., Simón-Sánchez, J., Schulte, C., Lesage, S., Sveinbjörnsdóttir, S., Stefánsson, K., Martinez, M., Hardy, S., Heutink, P., Brice, A., Gasser, T., Singleton, A. B., & Wood, N. W. (2011). Imputation of sequence variants for identification of genetic risks for Parkinson's disease: A meta-analysis of genome-wide association studies. *Lancet*, 377, 641–649. https://doi.org/10.1016/S0140-6736(10)62345-8

Kaeser, P. S., & Regehr, W. G. (2014). Molecular mechanisms for synchronous, asynchronous, and spontaneous neurotransmitter release. *Annual Review of Physiology*, 76, 333–363. https://doi.org/10.1146/annurev-physiol-021113-170338

Kavalali, E. T. (2015). The mechanisms and functions of spontaneous neurotransmitter release. *Nature Reviews Neuroscience*, 16, 5–16. https://doi.org/10.1038/nrn3875

Kavalali, E. T. (2018). Spontaneous neurotransmission: A form of neural communication comes of age. *Journal of Neuroscience Research*, 96, 331–334. https://doi.org/10.1002/jnr.24207

Kononenko, N. L., & Haucke, V. (2012). Spontaneous neurotransmission: a SNARE for the rest. *Neuron*, 73, 3–5. https://doi.org/10.1016/j.neuron.2011.12.015

Kullmann, D. M. (1994). Amplitude fluctuations of dual-component EPSCs in hippocampal pyramidal cells: implications for long-term potentiation. *Neuron*, 12, 1111–1120. https://doi.org/10.1016/0896-6273(94)90318-2

Liu, H., Dean, C., Arthur, C. P., Dong, M., & Chapman, E. R. (2009). Autapses and networks of hippocampal neurons exhibit distinct synaptic transmission phenotypes in the absence of synaptotagmin I. *Journal of Neuroscience*, 29, 7395–7403. https://doi.org/10.1523/JNEUROSCI.1341-09.2009

Mathew, S. S., Pozzo-Miller, L., & Hablitz, J. J. (2008). Kainate modulates presynaptic GABA release from two vesicle pools. *Journal of Neuroscience*, 28, 725–731. https://doi.org/10.1523/JNEUROSCI.3625-07.2008

Maximov, A., Shin, O. H., Liu, X., & Sudhof, T. C. (2007). Synaptotagmin-12, a synaptic vesicle phosphoprotein that modulates spontaneous neurotransmitter release. *Journal of Cell Biology*, 176, 113–124. https://doi.org/10.1083/jcb.200607021

Maximov, A., & Sudhof, T. C. (2005). Autonomous function of synaptotagmin 1 in triggering synchronous release independent of asynchronous release. *Neuron*, 48, 547–554. https://doi.org/10.1016/j.neuron.2005.09.006

Milochau, A., Lagree, V., Benassy, M. N., Chaignepain, S., Papin, J., Garcia-Arcos, I., Lajoix, A., Monterrat, C., Coudert, L., Schmitter, J. M., & Ochoa, B. (2014). Synaptotagmin 11 interacts with components of the RNA-induced silencing complex RISC in clonal pancreatic beta-cells. *FEBS Letters*, 588, 2217–2222.

Nishiki, T., & Augustine, G. J. (2004). Synaptotagmin I synchronizes transmitter release in mouse hippocampal neurons. *Journal of Neuroscience*, 24, 6127–6132. https://doi.org/10.1523/JNEUROSCI.1563-04.2004

Pallanck, L. (2003). A tale of two C2 domains. *Trends in Neurosciences*, 26, 2–4. https://doi.org/10.1016/S0166-2236(02)00007-3

Pang, Z. P., Bacaj, T., Yang, X., Zhou, P., Xu, W., & Sudhof, T. C. (2011). Doc2 supports spontaneous synaptic transmission by a Ca(2+)-independent mechanism. *Neuron*, 70, 244–251.

Pang, Z. P., & Sudhof, T. C. (2010). Cell biology of Ca^{2+}-triggered exocytosis. *Current Opinion in Cell Biology*, 22, 496–505. https://doi.org/10.1016/j.ceb.2010.05.001

Pang, Z. P., Sun, J., Rizo, J., Maximov, A., & Sudhof, T. C. (2006). Genetic analysis of synaptotagmin 2 in spontaneous and Ca^{2+}-triggered neurotransmitter release. *EMBO Journal*, 25, 2039–2050. https://doi.org/10.1038/sj.emboj.7601103

Pihlstrøm, L., Axelsson, G., Bjørnarå, K. A., Dizdar, N., Fardell, C., Forsgren, L., Holmberg, B., Larsen, J. P., Linder, J., Nissbrandt, H., Tysnes, O.-B., Öhman, E., Dietrichs, E., & Toft, M. (2013). Supportive evidence for 11 loci from genome-wide association studies in Parkinson's disease. *Neurobiology of Aging*, 34(6), 1708.e7–1708.e13. https://doi.org/10.1016/j.neurobiolaging.2012.10.019

Pratt, K. G., Zhu, P., Watari, H., Cook, D. G., & Sullivan, J. M. (2011). A novel role for γ-secretase: selective regulation of spontaneous neurotransmitter release from hippocampal neurons. *Journal of Neuroscience*, 31, 899–906.

Raingo, J., Khvotchev, M., Liu, P., Darios, F., Li, Y. C., Ramirez, D. M. O., Adachi, M., Lemieux, P., Toth, K., Davletov, B., & Kavalali, E. T. (2012). VAMP4 directs synaptic vesicles to a pool that selectively maintains asynchronous neurotransmission. *Nature Neuroscience*, 15, 738–745. https://doi.org/10.1038/nn.3067

Ramirez, D. M., Khvotchev, M., Trauterman, B., & Kavalali, E. T. (2012). Vti1a identifies a vesicle pool that preferentially recycles at rest and maintains spontaneous neurotransmission. *Neuron*, 73, 121–134. https://doi.org/10.1016/j.neuron.2011.10.034

Regehr, W. G. (2012). Short-term presynaptic plasticity. *Cold Spring Harbor Perspectives in Biology*, 4, a005702. https://doi.org/10.1101/cshperspect.a005702

Sara, Y., Virmani, T., Deak, F., Liu, X., & Kavalali, E. T. (2005). An isolated pool of vesicles recycles at rest and drives spontaneous neurotransmission. *Neuron*, 45, 563–573. https://doi.org/10.1016/j.neuron.2004.12.056

Schupp, M., Malsam, J., Ruiter, M., Scheutzow, A., Wierda, K. D., Sollner, T. H., & Sorensen, J. B. (2016). Interactions between SNAP-25 and synaptotagmin-1 are involved in vesicle priming, clamping spontaneous and stimulating evoked neurotransmission. *Journal of Neuroscience*, 36, 11865–11880. https://doi.org/10.1523/JNEUROSCI.1011-16.2016

Sesar, A., Cacheiro, P., López-López, M., Camiña-Tato, M., Quintáns, B., Monroy-Jaramillo, N., Alonso-Vilatela, M.-E., Cebrián, E., Yescas-Gómez, P., Ares, B., Rivas, M.-T., Castro, A., Carracedo, A., & Sobrido, M.-J. (2016). Synaptotagmin XI in Parkinson's disease: New evidence from an association study in Spain and Mexico. *Journal of the Neurological Sciences*, 362, 321–325. https://doi.org/10.1016/j.jns.2016.02.014

Shimojo, M., Madara, J., Pankow, S., Liu, X., Yates, J. 3rd, Sudhof, T. C., & Maximov, A. (2019). Synaptotagmin-11 mediates a vesicle trafficking pathway that is essential for development and synaptic plasticity. *Genes and Development*, 33, 365–376. https://doi.org/10.1101/gad.320077.118

Sreetama, S. C., Takano, T., Nedergaard, M., Simon, S. M., & Jaiswal, J. K. (2016). Injured astrocytes are repaired by Synaptotagmin XI-regulated lysosome exocytosis. *Cell Death and Differentiation*, 23, 596–607. https://doi.org/10.1038/cdd.2015.124

Sudhof, T. C., & Rothman, J. E. (2009). Membrane fusion: grappling with SNARE and SM proteins. *Science*, 323, 474–477. https://doi.org/10.1126/science.1161748

Sun, J., Pang, Z. P., Qin, D., Fahim, A. T., Adachi, R., & Sudhof, T. C. (2007). A dual-Ca^{2+}-sensor model for neurotransmitter release in a central synapse. *Nature*, 450, 676–682. https://doi.org/10.1038/nature06308

Takamori, S., Holt, M., Stenius, K., Lemke, E. A., Grønborg, M., Riedel, D., Urlaub, H., Schenck, S., Brügger, B., Ringler, P., Müller, S. A., Rammner, B., Gräter, F., Hub, J. S., De Groot, B. L., Mieskes, G., Moriyama, Y., Klingauf, J., Grubmüller, H., … Jahn, R. (2006). Molecular anatomy of a trafficking organelle. *Cell*, 127, 831–846. https://doi.org/10.1016/j.cell.2006.10.030

Truckenbrodt, S., & Rizzoli, S. O. (2014). Spontaneous vesicle recycling in the synaptic bouton. *Frontiers in Cellular Neuroscience*, 8, 409. https://doi.org/10.3389/fncel.2014.00409

von Poser, C., Ichtchenko, K., Shao, X., Rizo, J., & Sudhof, T. C. (1997). The evolutionary pressure to inactivate. A subclass of synaptotagmins with an amino acid substitution that abolishes Ca^{2+} binding. *Journal of Biological Chemistry*, 272, 14314–14319.

Walter, A. M., Kurps, J., de Wit, H., Schöning, S., Toft-Bertelsen, T. L., Lauks, J., Ziomkiewicz, I., Weiss, A. N., Schulz, A., Fischer von Mollard, G., & Verhage, M. (2014). The SNARE protein vti1a functions in dense-core vesicle biogenesis. *EMBO Journal*, 33, 1681–1697.

Wang, C., Kang, X., Zhou, L. I., Chai, Z., Wu, Q., Huang, R., Xu, H., Hu, M., Sun, X., Sun, S., Li, J., Jiao, R., Zuo, P., Zheng, L., Yue, Z., & Zhou, Z. (2018). Synaptotagmin-11 is a critical mediator of parkin-linked neurotoxicity and Parkinson's disease-like pathology. *Nature Communications*, 9, 81. https://doi.org/10.1038/s41467-017-02593-y

Wang, C., Wang, Y., Hu, M., Chai, Z., Wu, Q., Huang, R., Han, W., Zhang, C. X., & Zhou, Z. (2016). Synaptotagmin-11 inhibits clathrin-mediated and bulk endocytosis. *EMBO Reports*, 17, 47–63. https://doi.org/10.15252/embr.201540689

Wierda, K. D., & Sorensen, J. B. (2014). Innervation by a GABAergic neuron depresses spontaneous release in glutamatergic neurons and unveils the clamping phenotype of synaptotagmin-1. *Journal of Neuroscience*, 34, 2100–2110. https://doi.org/10.1523/JNEUROSCI.3934-13.2014

Williams, C. L., & Smith, S. M. (2018). Calcium dependence of spontaneous neurotransmitter release. *Journal of Neuroscience Research*, 96, 335–347. https://doi.org/10.1002/jnr.24116

Xu, J., Mashimo, T., & Sudhof, T. C. (2007). Synaptotagmin-1, -2, and -9: Ca(2+) sensors for fast release that specify distinct presynaptic properties in subsets of neurons. *Neuron*, 54, 567–581. https://doi.org/10.1016/j.neuron.2007.05.004

Xu, J., Pang, Z. P., Shin, O. H., & Sudhof, T. C. (2009). Synaptotagmin-1 functions as a Ca^{2+} sensor for spontaneous release. *Nature Neuroscience*, 12, 759–766. https://doi.org/10.1038/nn.2320

Yan, S., Wang, Y., Zhang, Y., Wang, L. E., Zhao, X., Du, C., Gao, P., Yan, F., Liu, F., Gong, X., Guan, Y., Cui, X., Wang, X., & Xi Zhang, C. (2020). Synaptotagmin-11 regulates the functions of caveolae and responds to mechanical stimuli in astrocytes. *The FASEB Journal*, 34, 2609–2624. https://doi.org/10.1096/fj.201901715R

Yang, X., Cao, P., & Sudhof, T. C. (2013). Deconstructing complexin function in activating and clamping Ca^{2+}-triggered exocytosis by comparing knockout and knockdown phenotypes. *Proceedings of the National Academy of Sciences*, 110, 20777–20782. https://doi.org/10.1073/pnas.1321367110